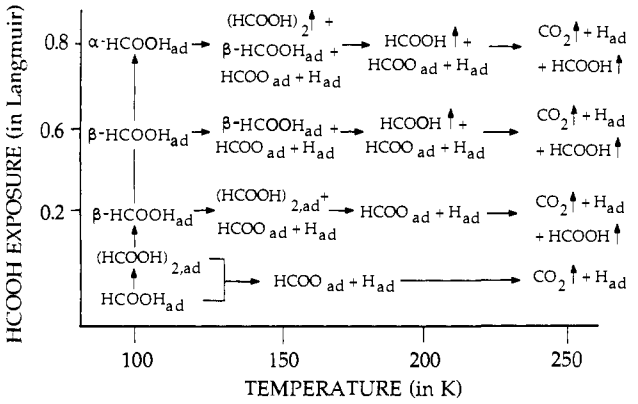

Figure 10. Summary of the coverage dependence of the HCOOH overlayer for adsorption at 80–100 K and its temperature dependence for conversion to formate for different coverages.

Rupture of the hydrogen-bonded chains via dimer displacement would result in a higher number of terminal HCOOH molecules. Chain rupture could be followed or accompanied by deprotonation of these terminal molecules; reorientation would be slowed by their continued interaction with linking HCOOH molecules in the shortened chains.

5. Conclusions

The scheme for the reaction of HCOOH with Pt(111) is summarized in Figure 10. For extremely low exposures at 80–100 K, we posit that HCOOH exists molecularly as monomers or discrete dimer pairs. As surface temperature increases, the acid deprotonates to produce bridging formate and hydrogen adatoms. As exposure increases at 80–100 K, the population of HCOOH reaches a level sufficient to form hydrogen-bonded chains in a configuration similar to the solid-phase β-polymorph. This is the surface condition we observe for an exposure of 0.2 L. Heating this overlayer to 150 K causes reversion to discrete dimer pairs, followed by conversion to bridging formate. By 170 K, conversion is complete. Between 200 K and 250 K a small amount of formate recombines with atomic hydrogen to desorb molecularly; however, the majority of formate decomposes, resulting in CO_2 desorption peaking at ~260 K.

We believe the β-polymorph remains the preferred configuration for HCOOH adsorbed at 80–100 K up to an exposure which populates the second molecular desorption state (0.6 L); however, at higher exposures the hydrogen-bonded chains resemble the denser α-polymorph. Heating the surface above 130 K transforms the α-phase to the β-phase; this is tied to the second molecular HCOOH desorption state. Desorption results from depopulation of a second layer or rupture of first-layer chains; the desorption products are gaseous dimers. A fraction of the HCOOH which remains in the overlayer immediately deprotonates and reorients to a perpendicular, bridging configuration with increasing surface temperature. The HCOOH which does not deprotonate desorbs from the surface (peaked at 200 K) as monomers.

Increasing exposure from 0.2 L to 0.6 L changes the pathway of formate formation. As described above for 0.2 L HCOOH exposure, production of formate is preceded by the reversion of HCOOH chains to discrete dimer pairs. Increasing coverage eventually prevents this reversion, leading to formate production directly from HCOOH chains and desorption of molecular HCOOH peaked at 200 K. Subsequent formate decomposition proceeds as for the 0.2 L exposure.

Acknowledgment is made to the donors of the Petroleum Research Fund, administered by the American Chemical Society, for the support of this research. Some equipment and all facilities are provided by the Ames Laboratory, which is operated for the U.S. Department of Energy by Iowa State University under Contract No. W-7405-ENG-82.

Registry No. HCOOH, 64-18-6; Pt, 7440-06-4; formate, 71-47-6.

Gas-Phase Oxidation of Group 6 Metal Carbonyl Anions

C. E. C. A. Hop† and T. B. McMahon*

Contribution from the Department of Chemistry and Guelph-Waterloo Centre For Graduate Work in Chemistry, University of Waterloo, Waterloo, Ontario N2L 3G1, Canada.
Received June 24, 1991

Abstract: Oxidation of $Cr(CO)_5^-$, $Mo(CO)_5^-$, and $W(CO)_5^-$ was examined in a low-pressure (~5×10^{-8} mbar) and a high-pressure (~3.5 mbar) environment using a Fourier-transform ion cyclotron resonance spectrometer equipped with a high-pressure external ion source. Although the oxidation chemistry displayed by the Cr and W systems was fairly similar, the Mo analogue had several unique features. In addition, remarkable differences were observed between high- and low-pressure oxidation. For example, MO_5^- ions were only generated under high-pressure conditions. This indicates that generation of MO_5^- ions requires termolecular reactions. Alternatively, it could be that the intermediate for generation of MO_5^- has a very short lifetime and dissociates prior to reaction with O_2 under low-pressure conditions. Energy-resolved collision-induced dissociation was used to obtain structural information about the various product ions, and it allowed determination of bond strengths in these ions. The experiments revealed that for all the $M(CO)_xO_2^-$ (x = 3, 4) product ions the two oxygen atoms are bound as two separate oxo ligands and not as a dioxygen ligand. The MO_5^- ions contain two (or possibly one) O_2 molecules bound as peroxo or superoxo ligands.

Introduction

Transitional metals play an important role in organic and inorganic chemistry and biochemistry.[1] The transition-metal oxides are of particular importance because of their involvement as catalysts in oxidation of organic substrates.[2] Transition-metal compounds containing a dioxygen ligand[3] are especially effective

† Present address: Department of Chemistry, University of Wisconsin—Madison, Madison, Wisconsin 53706.

(1) (a) Cotton, F. A.; Wilkinson, G. *Advanced Inorganic Chemistry*; John Wiley & Sons: New York, 1980. (b) Collman, J. P.; Hegedus, L. S.; Norton, J. R.; Finke, R. G. *Principles and Applications of Organotransition Metal Chemistry*; University Science Books: Mill Valley, 1987.

0002-7863/92/1514-1237$03.00/0

oxidants of organic substrates,[2] and they also play a crucial role in the storage and use of oxygen in biological systems.[2a,c,4] These properties are derived from the activation of dioxygen due to its coordination to the metal center. For a complete understanding of the processes involved, a detailed knowledge of the metal–oxygen bond is essential. Generally, mononuclear transition-metal dioxygen complexes can be divided into two groups: (1) side-on bidentate (η^2) peroxo (O_2^{2-}) compounds, **I**, and (2) end-on monodentate (η^1) superoxo (O_2^-) compounds, **II**.[1,3] These compounds can be compared with dioxo metal compounds, **III**.

$$\underset{\mathbf{I}}{M(\eta^2\text{-}O_2)} \qquad \underset{\mathbf{II}}{M(\eta^1\text{-}O_2)} \qquad \underset{\mathbf{III}}{M(O)_2}$$

Numerous transition-metal peroxo complexes have been synthesized and studied in detail.[2-8] The frequently explosive oxo diperoxo complexes of the group 6 metals, $MO(O_2)_2$ (M = Cr, Mo, W), are considered to be among the most reactive and they have frequently been used for oxidation of hydrocarbons, alcohols, aliphatic and aromatic amines, thiols,[5] and especially epoxidation of olefins.[6] Their structures have also been determined by X-ray crystallography.[3a,c,7] For example, $LCr(\eta^2\text{-}O_2)_2O$ with L = bipyridine exhibits a pentagonal bipyramidal structure.[7a] Several equilibrium and kinetic studies of oxo diperoxo complexes have been performed in solution in order to establish the formation and decomposition mechanisms of these complexes.[8]

The photooxidation of $M(CO)_6$ (M = Cr, Mo, W) has been studied extensively in a solid argon matrix doped with O_2.[9] Infrared and Raman spectroscopy was used to analyze the products and the following mechanism was proposed:

$$\begin{array}{ccccccc} & & & & & & M(CO)_4(O)_2 \\ & & & & & & \uparrow \\ M(CO)_6 & \longrightarrow & M(CO)_5 & \longrightarrow & M(CO)_4(\eta^2\text{-}O_2) & \longrightarrow & M(CO)_3(O)_2 \longrightarrow \\ M(CO)_2(O)_2 & \longrightarrow & M(O)_2 & \longrightarrow & M(O)_2(\eta^2\text{-}O_2) & \longrightarrow & M(O)_3 \end{array} \quad (1)$$

However, it should be noted that not all intermediates have been found for all three group 6 metals. The disadvantage of this IR technique is that the metal oxide molecules can also be perturbed due to their proximity to O_2 and the photoejected CO and CO_2 molecules present in the matrix, giving rise to uncertain vibrational assignments.

The gas phase lends itself particularly well to detailed studies of the structure and reactivity of transition-metal compounds, and with the advent of new experimental methods considerable progress has been made during the last 15 years.[10] Recently a few mass spectrometric studies have appeared which discuss the ion–molecule reactions of metal carbonyl anions with molecular oxygen.[11-13] Metal carbonyl anions are easily generated via dissociative electron attachment:[14]

$$M(CO)_x + e^- \rightarrow M(CO)_{x-1}^- + CO \quad (2)$$

Squires et al.[11] have used a flowing afterglow apparatus to show that the reactivity of the anions with oxygen is strongly dependent on the nature of the metal atom. The three main reaction pathways observed were

$$M(CO)_y^- + O_2 \rightarrow M(CO)_{y-1}O_2^- + CO \quad (3)$$

$$M(CO)_y^- + O_2 \rightarrow M(CO)_{y-2}O_2^- + 2\,CO \quad (4)$$

$$M(CO)_y^- + O_2 \rightarrow M(CO)_{y-2}O^- + CO + CO_2 \quad (5)$$

$Cr(CO)_5^-$, $W(CO)_5^-$, and $Fe(CO)_4^-$ reacted predominantly via pathway 5, producing $Cr(CO)_3O^-$, $W(CO)_3O^-$, and $Fe(CO)_2O^-$, respectively. In marked contrast, this process did not take place for $Mo(CO)_5^-$. Instead, $Mo(CO)_5^-$ yielded $Mo(CO)_4O_2^-$ and $Mo(CO)_3O_2^-$ via reactions 3 and 4. $Ni(CO)_3^-$ almost exclusively displayed displacement of one CO ligand by O_2. The data for the three group 6 transition-metal carbonyl anions are summarized in Table I. At higher oxygen concentrations the spectra were dominated by polyoxide ions, MO_z^- (z = 2, 3, 4, 5). The structures of primary and terminal product ions were not established. However, for the polyoxide ions rare oxidation states and/or oxygen bonding modes were suggested. For example, by analogy with data from the matrix isolation studies dioxo structures were suggested for $M(CO)_3O_2^-$ (M = Cr, Mo).

Recently Bricker et al.[12] have examined the ion–molecule reactions of $Cr(CO)_5^-$ with O_2 in the low-pressure environment of a Fourier-transform ion cyclotron resonance (FT-ICR) spectrometer. Generally, the results were in good agreement with those of Squires et al.[11] with the primary product ions being $Cr(CO)_3O^-$ and $Cr(CO)_3O_2^-$. Oxidation of $Cr(CO)_3O^-$ produced CrO_3^-, but no CrO_2^-, CrO_4^-, or CrO_5^- ions were observed. The $Cr(CO)_3O_2^-$ and CrO_3^- ions did not react with O_2. Structural information for the product ions was obtained via collision-induced dissociation

Table I. Products from the Reactions of Group 6 Metal Carbonyl Anions with Molecular Oxygen[a]

$M(CO)_5^-$	primary product ions	terminal ions
$Cr(CO)_5^-$	$Cr(CO)_3O^-$ (95%)	CrO_x^- (x = 2–5)
	$Cr(CO)_3O_2^-$ (5%)	$Cr(CO)_3O_2^-$
$Mo(CO)_5^-$	$Mo(CO)_3O_2^-$ (55%)	MoO_x^- (x = 3–4)
	$Mo(CO)_4O_2^-$ (45%)	
$W(CO)_5^-$	$W(CO)_3O^-$ (56%)	WO_x^- (x = 2–5)
	$W(CO)_3O_2^-$ (20%)	
	$W(CO)O_2^-$ (13%)	
	$W(CO)_2O_2^-$ (10%)	
	$W(CO)_4O_2^-$ (1%)	

[a] From ref 11b.

(2) (a) Spiro, T. G., Ed. *Metal Ion Activation of Dioxygen*; John Wiley & Sons: New York, 1980. (b) Sheldon, R. A.; Kochi, J. K. *Metal-Catalyzed Oxidations of Organic Compounds*; Academic Press: New York, 1981. (c) Martell, A. E.; Sawyer, D. T., Eds. *Oxygen Complexes and Oxygen Activation by Transition Metals*; Plenum Press: New York, 1988.

(3) (a) Vaska, L. *Acc. Chem. Res.* **1976**, *9*, 175. (b) Lever, A. B. P.; Gray, H. B. *Acc. Chem. Res.* **1978**, *11*, 348. (c) Gubelmann, M. H.; Williams, A. F. *Struct. Bonding (Berlin)* **1983**, *55*, 1.

(4) (a) Jones, R. D.; Summerville, D. A.; Basolo, F. *Chem. Rev.* **1979**, *79*, 139. (b) Niederhoffer, E. C.; Timmons, J. H.; Martell, A. E. *Chem. Rev.* **1984**, *84*, 137.

(5) (a) Vedejs, E. *J. Am. Chem. Soc.* **1974**, *96*, 5944. (b) Fleet, G. W. J.; Little, W. *Tetrahedron Lett.* **1977**, *42*, 3749. (c) Jacobsen, S. E.; Muccigrosso, D. A.; Mares, F. *J. Org. Chem.* **1979**, *44*, 921. (d) Daire, E.; Mimoun, H.; Saussine, L. *Nouv. J. Chim.* **1984**, *8*, 271. (e) Firouzabadi, H.; Iranpoor, N.; Kiaeezadeh, F.; Toofan, J. *Tetrahedron* **1986**, *42*, 719.

(6) (a) Mimoun, H.; De Roch, I. S.; Sajies, L. *Tetrahedron* **1970**, *26*, 37. (b) Chong, A. O.; Sharpless, K. B. *J. Org. Chem.* **1977**, *42*, 1587. (c) Mimoun, H. *J. Mol. Catal.* **1980**, *7*, 1. (d) Mimoun, H. In *The Chemistry of Functional Group Peroxides*; Patai, S., Ed.; Interscience: New York, 1983. (e) Chaumette, P.; Mimoun, H.; Saussine, L.; Fischer, J.; Mitschler, A. *J. Organomet. Chem.* **1983**, *250*, 291.

(7) (a) Conner, J. A.; Ebsworth, E. A. V. *Adv. Inorg. Chem. Radiochem.* **1964**, *6*, 279 and references herein. (b) Stomberg, R.; Ainalem, I.-B. *Acta Chem. Scand.* **1968**, *22*, 1439. (c) Jacobsen, S. E.; Tang, R.; Mares, F. *Inorg. Chem.* **1978**, *17*, 3055 and references herein. (d) Dengel, A. C.; Griffith, W. P.; Powell, R. D.; Skapski, A. C. *J. Chem. Soc., Dalton Trans.* **1987**, 991 and references herein.

(8) (a) Funahashi, S.; Uchida, F.; Tanaka, M. *Inorg. Chem.* **1978**, *17*, 2784. (b) Lydon, J. D.; Schwane, L. M.; Thompson, R. C. *Inorg. Chem.* **1987**, *26*, 2606. (c) Ghiron, A. F.; Thompson, R. C. *Inorg. Chem.* **1988**, *27*, 4766. (d) Schwane, L. M.; Thompson, R. C. *Inorg. Chem.* **1989**, *28*, 3938.

(9) (a) Poliakoff, M.; Smith, K. P.; Turner, J. J.; Wilkinson, A. J. *J. Chem. Soc., Dalton Trans.* **1982**, 651. (b) Crayston, J. A.; Almond, M. J.; Downs, A. J.; Poliakoff, M.; Turner, J. J. *Inorg. Chem.* **1984**, *23*, 3051. (c) Almond, M. J.; Crayston, J. A.; Downs, A. J.; Poliakoff, M.; Turner, J. J. *Inorg. Chem.* **1986**, *25*, 19. (d) Almond, M. J.; Downs, A. J. *J. Chem. Soc., Dalton Trans.* **1988**, 809.

(10) (a) Russell, D. H., Ed. *Gas Phase Inorganic Chemistry*; Plenum Press: New York, 1989. (b) Marks, T. J., Ed. *Bonding Energetics in Organometallic Compounds*; American Chemical Society: Washington, DC, 1990.

(11) (a) Lane, K.; Sallans, L.; Squires, R. R. *J. Am. Chem. Soc.* **1984**, *106*, 2719. (b) Squires, R. R. *Chem. Rev.* **1987**, *87*, 623.

(12) Bricker, D. L.; Russell, D. H. *J. Am. Chem. Soc.* **1987**, *109*, 3910.

(13) (a) McDonald, R. N.; Chowdhury, A. K.; Jones, M. T. *J. Am. Chem. Soc.* **1986**, *108*, 3105. (b) McDonald, R. N.; Schell, P. L. *Organometallics* **1988**, *7*, 1806. (c) McDonald, R. N.; Schell, P. L. *Organometallics* **1988**, *7*, 1820.

(14) George, P. M.; Beauchamp, J. L. *J. Chem. Phys.* **1982**, *76*, 2959.

(CID).[15] Loss of O_2 upon collisional activation of $Cr(CO)_3O_2^-$ was interpreted as evidence for a structure containing O_2 as an end-on superoxo or side-on peroxo ligand, rather than a dioxo structure as suggested by Squires et al.[11a] $Cr(CO)_3O^-$ lost CO upon collisional activation.

In the present study the oxidation of $Cr(CO)_5^-$, $Mo(CO)_5^-$, and $W(CO)_5^-$ ions was investigated in both a low-pressure and a high-pressure ($\sim 5 \times 10^{-8}$ and ~ 3.5 mbar, respectively) environment using a FT-ICR spectrometer with a high-pressure external ion source. Structural information for the product ions was obtained via collision-induced dissociation and ion–molecule reactions. In addition, to add to our knowledge of metal–carbon and metal–oxygen bonds, bond strengths in the oxidized product ions were measured using threshold CID techniques.[16-18]

Experimental Section

All experiments were performed with a Bruker Spectrospin CMS 47 Fourier-transform ion cyclotron resonance spectrometer[19a] equipped with a high-pressure external ion source.[19b] $Cr(CO)_6$, $Mo(CO)_6$, and $W(CO)_6$ were used as precursors to the metal carbonyl anions and CH_4 was the inert bath gas in the high-pressure ion source. Chemical ionization pressures up to 4 mbar and 2 keV electrons were used for ionization. Average ion residence times in the high-pressure ion source were on the order of 5 ms. The temperature of the high-pressure ion source was ~ 30 °C. Addition of a small amount of O_2 to the mixture introduced into the external ion source induced oxidation of the metal carbonyl anions. Gas flow restrictions and differential pumping provided a pressure differential of 10^9 between the external ion source and the ICR cell. For example, for a typical pressure inside the ion source of 4 mbar, the pressure in the ICR cell was 4×10^{-9} mbar, principally CH_4. The product ions were transferred from the high-pressure ion source to the low-pressure ICR cell and trapped, followed by a 2-s delay to thermalize the ions by collision with argon present in the ICR cell at 5.0×10^{-8} mbar. Ejection of all other ions from the ICR cell resulted in isolation of the ion of interest. A radio frequency pulse at the exact cyclotron frequency was then used to increase the translational energy of this ion to a known value. The amplitude and duration of the radio frequency pulse determined the translational energy of the ion.[18] In our experiments the amplitude was fixed and the duration of the radio frequency pulse was variable. In the subsequent delay, collision-induced dissociation took place with argon as the target gas. The fragment ions were detected in both broad band mode (full mass spectrum) and narrow band mode (single ion detection with high mass resolution). Each experiment was repeated 16 times to obtain a good signal-to-noise ratio. For threshold energy measurements the fragment ion intensity was measured in the narrow band mode as a function of the center-of-mass energy of the parent ion.[18] The length of the CID delay was 10 ms, which corresponds to single-collision conditions.[18a] The shape of the curve representing the center-of-mass energy, E_{cm}, dependence of the fragment ion intensity was analyzed with an empirical model, eq 6,[16] where E_t is the threshold energy of the endothermic reaction, σ_0 is an energy-independent scaling factor, and n and m are variables. In this study we restricted analysis to $m = 1$ while the

$$\sigma(E_{cm}) = \sigma_0(E_{cm} - E_t)^n / E_{cm}^m \quad (6)$$

other parameters, σ_0, E_t, and n, were optimized by using a nonlinear least-squares analysis to give the best fit to the experimental data. Armentrout et al.[16] have found that the form with $m = 1$ is one of the most useful in deriving accurate thermochemistry. In addition, this form has been predicted theoretically for translationally driven reactions.[20]

Alternatively, ion activation can be omitted in the procedure described above, and the reactivity of the isolated ions with certain substrates, such as O_2 and NO, can be examined by varying the delay between isolation of the ion of interest and detection.

Unless otherwise stated, the CID and reactivity experiments were performed with ions containing the ^{52}Cr, ^{98}Mo, or ^{186}W isotopes, whose natural abundances are 83.76%, 24.00%, and 28.64%, respectively.

All compounds were of commercial origin and showed no detectable impurities. $^{18}O_2$ (97.7 atom % ^{18}O) was purchased from MSD Isotopes.

Results

A. Oxidation of $Cr(CO)_5^-$. The only ion of significant abundance generated upon admission of a mixture of CH_4 and $Cr(CO)_6$ vapor to the external ion source was $Cr(CO)_5^-$. Oxidation of $Cr(CO)_5^-$ was performed in two ways: (i) in the high-pressure external ion source and (ii) in the low-pressure ICR cell.

Adding O_2 to the mixture introduced to the high-pressure ion source caused a rapid decrease in the intensity of $Cr(CO)_5^-$ and the appearance of $Cr(CO)_3O_2^-$ and $Cr(CO)_3O^-$ ions. In the presence of 0.7% O_2 the relative abundances of $Cr(CO)_5^-$, $Cr(CO)_3O_2^-$, $Cr(CO)_3O^-$, CrO_5^-, and CrO_3^- were 100, 4, 80, 6, and 0.7, respectively. Approximately 1% of O_2 in the mixture was sufficient for CrO_5^- to become the base peak of the mass spectrum, and with 1.3% O_2 the relative abundances of the above ions were 10, 2, 37, 100, and 2, respectively. Admission of more O_2 to the mixture caused the disappearance of all mono-chromium ions except CrO_5^-. It is worth noting that with an O_2 content as high as 70% CrO_5^- was still the base peak of the spectrum despite a significant decrease in its absolute abundance. Although there are some differences in terminal ions (see below), the agreement with the flowing afterglow data (Table I) is good.

At O_2 concentrations above 0.7% ions containing more than one chromium atom were formed as well: $Cr_2(CO)_xO^-$ ($x = 6$–9), $Cr_2(CO)_xO_2^-$ ($x = 5$, 6), $Cr_2(CO)_xO_3^-$ ($x = 3$, 4, 6), $Cr_2O_x^-$ ($x = 4$–7), and $Cr_3O_x^-$ ($x = 8$, 10). The abundance of most of the latter ions was rather low and they resulted from interaction between chromium-containing ions and neutral $Cr(CO)_6$. These ions will not be considered in detail here.

When $Cr(CO)_5^-$ ions were trapped in the ICR cell in the presence of 5.0×10^{-8} mbar of O_2 for extended periods of time (Figure 1A), the FT-ICR results of Bricker et al.[12] were well reproduced:

$$Cr(CO)_5^- + O_2 \rightarrow Cr(CO)_3O_2^- + 2\,CO \quad (7)$$

$$Cr(CO)_5^- + O_2 \rightarrow Cr(CO)_3O^- + CO + CO_2 \quad (8)$$

Predictably, the presence of $^{18}O_2$ in the ICR cell resulted in generation of $Cr(CO)_3{}^{18}O_2^-$ and $Cr(CO)_3{}^{18}O^-$. The first step in the generation of these products is most likely the generation of a superoxide anion by radical–radical interaction between the initial 17-electron radical anion and triplet O_2.[11,13] The $Cr(CO)_3O^-$:$Cr(CO)_3O_2^-$ ratio increased slightly with increased reaction time of the $Cr(CO)_5^-$ ions, rising from 6.4:1 after 4 s to 7.7:1 after 30 s. Externally generated $Cr(CO)_3O^-$ and $Cr(CO)_3O_2^-$ ions produced CrO_3^- upon interaction with O_2 in the ICR cell; 20 s after individual isolation of these ions CrO_3^- was 29% of the total ion signal in the former case and 21% in the latter case.

$$Cr(CO)_3O^- + O_2 \rightarrow CrO_3^- + 3\,CO \quad (9)$$

$$Cr(CO)_3O_2^- + O_2 \rightarrow CrO_3^- + 2\,CO + CO_2 \quad (10)$$

CrO_5^- did not display any reactivity toward O_2. To examine the possibility of displacement of oxygen ligands, CrO_5^- ions were trapped in an $^{18}O_2$ environment. No inclusion of ^{18}O atoms was observed, even after very long reaction delays.

$$Cr^{16}O_5^- + {}^{18}O_2 \rightarrow \text{no reaction} \quad (11)$$

Energy-resolved CID was used to assess the structure of the product ions. The CID mass spectra of some of the product ions are presented in Table II. Bond dissociation energies for the dissociation processes of lowest energy requirement were obtained

(15) (a) Holmes, J. L. *Org. Mass Spectrom.* **1985**, *20*, 169. (b) Busch, K. L.; Glish, G. L.; McLuckey, S. A. *Mass Spectrometry/Mass Spectrometry. Techniques and Applications of Tandem Mass Spectrometry*; VCH: New York, 1988.

(16) (a) Sunderlin, L.; Aristov, N.; Armentrout, P. B. *J. Am. Chem. Soc.* **1987**, *109*, 78 and references therein. (b) Boo, B. H.; Armentrout, P. B. *J. Am. Chem. Soc.* **1987**, *109*, 3549. (c) Aristov, N.; Armentrout, P. B. *J. Chem. Phys.* **1987**, *91*, 6178. (d) Sunderlin, L. S.; Armentrout, P. B. *J. Am. Chem. Soc.* **1989**, *111*, 3845. (e) Boo, B. H.; Elkind, J. L.; Armentrout, P. B. *J. Am. Chem. Soc.* **1990**, *112*, 2083 and references therein.

(17) (a) Graul, S. T.; Squires, R. R. *J. Am. Chem. Soc.* **1989**, *111*, 892. (b) Graul, S. T.; Squires, R. R. *J. Am. Chem. Soc.* **1990**, *112*, 2517. (c) Graul, S. T.; Squires, R. R. *Int. J. Mass Spectrom. Ion Processes* **1990**, *100*, 785 and references therein.

(18) (a) Hop, C. E. C. A.; McMahon, T. B.; Willett, G. D. *Int. J. Mass Spectrom. Ion Processes* **1990**, *101*, 191. (b) Hop, C. E. C. A.; McMahon, T. B. *J. Am. Chem. Soc.* **1991**, *113*, 355. (c) Hop, C. E. C. A.; McMahon, T. B. *Inorg. Chem.* **1991**, *30*, 2828.

(19) (a) Alleman, M.; Kellerhals, H.-P.; Wanczek, K. P. *Int. J. Mass Spectrom. Ion Phys.* **1983**, *46*, 139. (b) Kofel, P.; McMahon, T. B. *Int. J. Mass Spectrom. Ion Processes* **1990**, *98*, 1.

(20) Chesnavich, W. J.; Bowers, M. T. *J. Phys. Chem.* **1979**, *83*, 900.

Table II. Collision-Induced Dissociation (CID) Mass Spectra of Various ^{52}Cr-, ^{98}Mo-, or ^{186}W-Containing Anions Having a Center-of-Mass Energy of 10.0 eV[a]

parent ion	neutral species lost upon CID (relative intensity)			
$Cr(CO)_5^-$	CO (11)	2 CO (3)		
	CO (39)	*2 CO (13)*	*3 CO (3)*	*4 CO (0.5)*
$Cr(CO)_3O_2^-$[b]	3 CO (7)			
	2 CO (8)	*3 CO (46)*		
$Cr(CO)_3O^-$	CO (8)	2 CO (4)		
	CO (23)	*2 CO (13)*	*3 CO (2)*	*[C_3,O_4] (0.8)*
CrO_5^-	O_2 (9)			
	O_2 (41)	*[O_3] (0.9)*	*[O_5] (0.8)*	
$Mo(CO)_5^-$	CO (12)	2 CO (3)		
	CO (40)	*2 CO (20)*	*3 CO (3)*	
$Mo(CO)_4O_2^-$	CO (6)	3 CO (7)	4 CO (4)	
	CO (23)	*3 CO (33)*	*4 CO (22)*	
$Mo(CO)_3O_2^-$	2 CO (8)	3 CO (11)		
	2 CO (42)	*3 CO (67)*		
MoO_5^-	O_2 (7)			
	O (3)	*O_2 (28)*		
$W(CO)_5^-$	CO (15)	2 CO (4)		
	CO (50)	*2 CO (24)*	*3 CO (4)*	*4 CO (1)*
$W(CO)_4O_2^-$	3 CO (22)	4 CO (12)		
	3 CO (194)	*4 CO (117)*		
$W(CO)_3O_2^-$	2 CO (16)	3 CO (15)		
	2 CO (84)	*3 CO (91)*		
$W(CO)O_2^-$[c]	CO (12)			
	CO (53)			
$W(CO)_3O^-$	CO (11)	2 CO (2)		
	CO (41)	*2 CO (15)*	*3 CO (3)*	
WO_5^-	O (1)	O_2 (10)		
	O (4)	*O_2 (37)*		
WO_4^-[d]	O (13)			
	O (57)			
WO_3^-[d]	O (14)			
	O (36)			

[a] Argon is the target and the CID interaction time is 50 ms. The data for a CID interaction time of 200 ms (multiple-collision conditions) are presented in italics. The intensity of the fragment ions is relative to that of the parent ions (=100). [b] The mass spectrum of all externally generated ions showed that 12% of the m/z 168 ions had the $Cr_2O_4^-$ structure. However, the absolute intensity of the CrO_2^- fragment ions in the CID mass spectrum obtained with a delay of 200 ms was considerably higher than that of the $Cr_2O_4^-$ ions in the mass spectrum of all externally generated ions, which implies that most of the CrO_2^- fragment ions must be due to dissociation of $Cr(CO)_3O_2^-$ and not $Cr_2O_4^-$. [c] The experiment was performed with $^{184}W(CO)O_2^-$ to prevent interference from WO_4^-. [d] The center-of-mass energy of the ions was 100 eV.

Table III. Threshold Energies of the Collision-Induced Dissociation (CID) Processes of Lowest Energy Requirement for Various ^{52}Cr-, ^{98}Mo-, or ^{186}W-Containing Anions[a]

parent ion	neutral species lost upon CID	threshold energy, E_t,[c] eV	n[c]
$Cr(CO)_5^-$	CO	1.94 ± 0.15	1.88 ± 0.10
$Cr(CO)_3O_2^-$[b]	2CO	1.22 ± 0.10	1.97 ± 0.10
$Cr(CO)_3O^-$	CO	1.65 ± 0.15	1.85 ± 0.10
CrO_5^-	O_2	1.33 ± 0.15	1.73 ± 0.05
$Mo(CO)_5^-$	CO	1.80 ± 0.10	1.76 ± 0.05
$Mo(CO)_4O_2^-$	CO	0.60 ± 0.05	1.70 ± 0.05
$Mo(CO)_3O_2^-$[b]	2CO	0.42 ± 0.05	1.41 ± 0.05
MoO_5^-[b]	O_2	1.52 ± 0.20	1.93 ± 0.20
$W(CO)_5^-$	CO	1.65 ± 0.10	1.94 ± 0.10
$W(CO)_3O_2^-$	2CO	≤ 0.10	1.88 ± 0.05
$W(CO)_3O^-$	CO	1.66 ± 0.10	1.86 ± 0.05
WO_5^-	O_2	1.77 ± 0.15	1.75 ± 0.10

[a] These data and the corresponding n values were obtained by analyzing the center-of-mass energy dependence of the fragment ion abundance with eq 6. Argon is the target and the CID interaction time is 10 ms, which corresponds with single-collision conditions.[17] [b] A CID interaction time of 25 ms was used because of the low intensity of the parent ion signal. [c] Error bars for the threshold and n values are obtained from a number of replicate determinations of the same threshold and individual nonlinear least-squares analysis of the data.

Table IV. Collision-Induced Dissociation (CID) Mass Spectra of $^{52}Cr^{16}O_x{}^{18}O_y^-$ ($x + y = 5$) Anions Having a Center-of-Mass Energy of 10.0 eV[a]

parent ion	neutral species lost upon CID (relative intensity)		
$Cr^{16}O_5^-$	$^{16}O_2$ (9)		
	$^{16}O_2$ (41)		
$Cr^{16}O_4{}^{18}O^-$	$^{16}O_2$ (10)	$^{16}O^{18}O$ (1)	
	$^{16}O_2$ (46)	*$^{16}O^{18}O$ (5)*	
$Cr^{16}O_3{}^{18}O_2^-$	$^{16}O_2$ (5)	$^{16}O^{18}O$ (1)	$^{18}O_2$ (5)
	$^{16}O_2$ (20)	*$^{16}O^{18}O$ (4)*	*$^{18}O_2$ (22)*

[a] Argon is the target and the CID interaction time is 50 ms. The data for a CID interaction time of 200 ms are presented in italics. The intensity of the fragment ions is relative to that of the parent ions (=100).

from threshold curves and are listed in Table III. A typical threshold curve for the collision-induced loss of CO from $Cr(CO)_5^-$ is shown in Figure 2.

For all CO-containing ions (including those containing two chromium atoms) the least energy demanding process was loss of one or more CO molecules. The CO binding energy in $Cr(CO)_5^-$ was determined to be 1.94 ± 0.15 eV, which is only slightly higher than that obtained via energy-resolved CID in a triple quadrupole, 1.86 ± 0.17 eV.[21] An earlier electron impact study gave a threshold value of only 0.5 eV.[22] Significantly, loss of O_2 was not observed for $Cr(CO)_3O_2^-$. In contrast, Bricker et al.[12] did observe O_2 loss from the latter ions; however, initially the two sets of data were not considered to necessarily contradict each other. Bricker et al.[12] had recorded the CID mass spectrum of $Cr(CO)_3O_2^-$ ions resulting from oxidation of $Cr(CO)_5^-$ ions in the (low-pressure) ICR cell while in the present experiments the $Cr(CO)_3O_2^-$ generated in a high-pressure ion source were sampled. Therefore we performed an MS/MS/MS experiment in which externally generated $Cr(CO)_5^-$ ions were isolated and allowed to react with O_2. This was followed by isolation of the $Cr(CO)_3O_2^-$ product ions and acceleration of these ions via a radio frequency pulse. The resulting CID mass spectrum was identical to that of $Cr(CO)_3O_2^-$ ions generated in the high-pressure source (Table II); no loss of O_2 was observed. The discrepancy with the results of Bricker et al.[12] is striking and cannot be explained. It should be noted that photooxidation of $Cr(CO)_6$ in solid argon produced only $Cr(CO)_3O_2$ species having the dioxo structure.[9]

The CrO_5^- ions lost O_2 upon collisional activation with the O_2 ligand being bound by 1.33 ± 0.15 eV. The latter value is, to our knowledge, the first metal–O_2 binding energy presented in the literature. At a higher center-of-mass energy (>15 eV) CrO_2^- was observed as well, but loss of (nominally) two O_2 molecules did not occur. Therefore, the CrO_3^- fragment ions from CrO_5^- could have the trioxo structure. Admission of a mixture of $^{16}O_2$ and $^{18}O_2$ (11:4) to the external ion source resulted in the generation of (among others) $Cr^{16}O_4{}^{18}O^-$ and $Cr^{16}O_3{}^{18}O_2^-$ ions. The CID mass spectra of these ions, presented in Table IV, show that the loss of mono-isotopic dioxygen ($^{16}O_2$,$^{18}O_2$) dominates.

Like the neutral oxo diperoxo complexes,[5,6] the CrO_5^- ions displayed oxidative properties. Trapping CrO_5^- ions in an NO environment resulted in oxygen abstraction:

$$CrO_5^- + NO \rightarrow CrO_4^- + NO_2 \qquad \Delta H^\circ_{rxn} = -39\ \text{kJ·mol}^{-1}\ [23\text{–}25] \qquad (12)$$

After 20 s the CrO_4^- ions represented 54% of the total ion intensity,

(21) Squires, R. R. Private communication, 1990.
(22) Pignataro, S.; Foffani, A.; Grasso, F.; Cantone, B. *Z. Phys. Chem. Neue Folge* **1965**, *47*, 106.
(23) $\Delta H_f(NO)$ and $\Delta H_f(NO_2)$ from: Lias, S. G.; Bartmess, J. E.; Liebman, J. F.; Holmes, J. L.; Levin, R. D.; Mallard, W. G. *J. Phys. Chem. Rev. Data* **1988**, *17*, Suppl. 1.
(24) $\Delta H_f(CrO_4^-)$ from: Rudnyi, E. B.; Vovk, O. M.; Kaibicheva, E. A.; Sidorov, L. N. *J. Chem. Thermodyn.* **1989**, *21*, 247.
(25) The heat of formation of CrO_5^-, −800 kJ·mol^{-1}, was obtained from $\Delta H_f(CrO_3^-)$ = −669 kJ·mol^{-1} [24] and the measured bond dissociation energy for loss of O_2 from CrO_5^-, 1.36 eV.

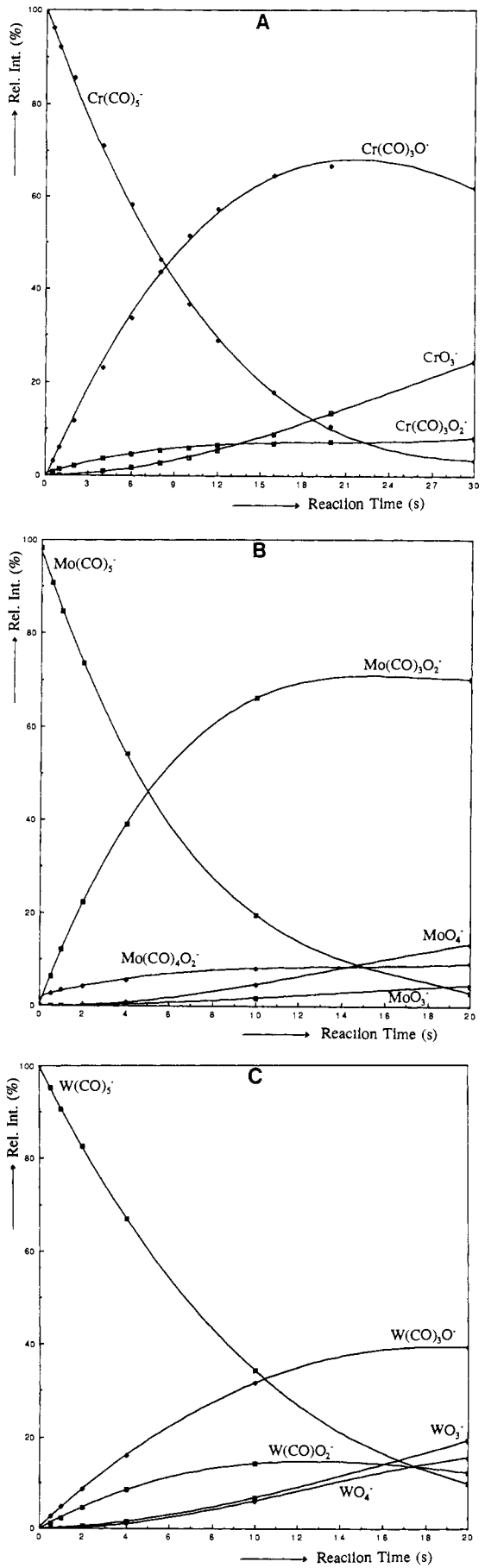

Figure 1. Temporal variation of the abundance of the product ions resulting from oxidation of $Cr(CO)_5^-$ (A), $Mo(CO)_5^-$ (B), and $W(CO)_5^-$ (C) with O_2 (5×10^{-8} mbar) in the ICR cell.

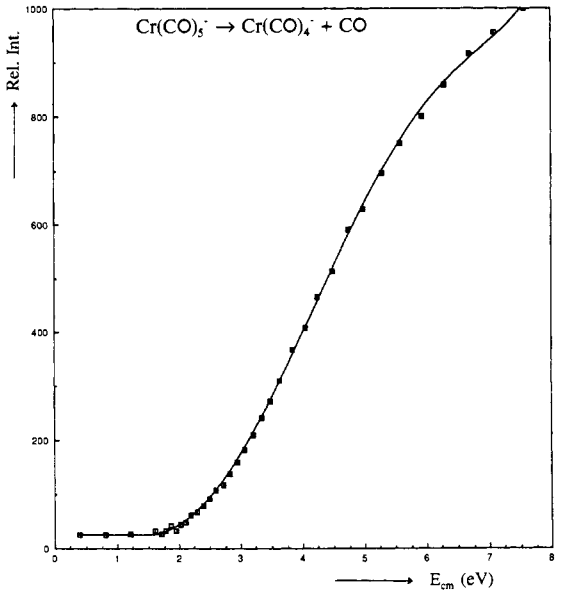

Figure 2. Center-of-mass energy dependence for the collision-induced loss of CO from isolated $Cr(CO)_5^-$ ions with Ar as target (5×10^{-8} mbar) and a 10-ms interaction time (single-collision conditions). The y-axis represents the ratio of the intensities of the fragment and parent ions normalized to 1000 for the ratio at a center-of-mass energy of 7.6 eV. The ratio of intensities does not go to zero at energies below threshold due to the nature of the algorithm which calculates peak areas. No peak is observable above the noise at these low energies, and at energies above threshold the signal-to-noise ratio of the data may be obtained from the intensity relative to that at low energy.

indicating a relatively slow reaction.

B. Oxidation of $Mo(CO)_5^-$. $Mo(CO)_5^-$ was obtained via dissociative electron attachment to $Mo(CO)_6$. As little as 0.2% O_2 in the mixture admitted to the high-pressure ion source was sufficient for $Mo(CO)_4O_2^-$ to become the base peak in the mass spectrum. With 0.4% O_2 the relative intensities of $Mo(CO)_5^-$ and the primary product ions $Mo(CO)_4O_2^-$ and $Mo(CO)_3O_2^-$ were 64, 100, and 18, respectively. The latter spectrum differs markedly from that obtained for the chromium analogue under similar circumstances. Increasing the O_2 content caused a decrease in the relative intensities of $Mo(CO)_5^-$ and $Mo(CO)_3O_2^-$, while MoO_5^- and MoO_4^- signals appeared. In the presence of 1.2% O_2 the relative intensities of $Mo(CO)_5^-$, $Mo(CO)_4O_2^-$, $Mo(CO)_3O_2^-$, MoO_5^-, and MoO_4^- were 2, 100, 6, 3, and 1, respectively. The relative abundance of the $Mo(CO)_4O_2^-$ and $Mo(CO)_3O_2^-$ ions differs significantly from that observed by Squires et al.[11b] in flowing afterglow experiments (Table I) where $Mo(CO)_3O_2^-$ was the most intense primary product ion. In contrast to the chromium and tungsten analogues, with a 65% O_2 content $Mo(CO)_4O_2^-$ was still the base peak in the spectrum with the relative intensities of $Mo(CO)_4O_2^-$, MoO_5^-, and MoO_4^- being 100, 19, and 18, respectively. (Under the latter conditions the absolute abundance of all ions was reduced markedly.) MoO_5^- was not observed by Squires et al.[11b]

At higher O_2 concentrations (>1%) ions containing two or more molybdenum atoms (e.g. $Mo_2O_x^-$, $x = 6$–8) were formed as well.

The results from low-pressure (5.0×10^{-8} mbar) oxidation of $Mo(CO)_5^-$ in the ICR cell are presented in Figure 1B. The primary product ions were $Mo(CO)_4O_2^-$ and $Mo(CO)_3O_2^-$, whereas $Mo(CO)_3O^-$ ions were not detected.

$$Mo(CO)_5^- + O_2 \rightarrow Mo(CO)_4O_2^- + CO \quad (13)$$

$$Mo(CO)_5^- + O_2 \rightarrow Mo(CO)_3O_2^- + 2CO \quad (14)$$

While $Mo(CO)_4O_2^-$ dominated high-pressure oxidation, at low pressure $Mo(CO)_3O_2^-$ was the most prevalent product ion. The flowing afterglow data (Table I) represent an intermediate situation. The $Mo(CO)_4O_2^-$ and MoO_5^- ions generated in the external source did not react with O_2. The $Mo(CO)_3O_2^-$ ions slowly reacted with O_2 producing MoO_4^- and MoO_3^-; after 20 s the MoO_4^- and

MoO_3^- ions represented 22 and 14% respectively of the total ion abundance.

$$Mo(CO)_3O_2^- + O_2 \rightarrow MoO_4^- + 3\,CO \quad (15)$$

$$Mo(CO)_3O_2^- + O_2 \rightarrow MoO_3^- + 2\,CO + CO_2 \quad (16)$$

The $Mo(CO)_5^-$ ions lost CO upon collisional activation (Table II), and a threshold measurement revealed that the metal–CO bond strength is somewhat weaker than that in $Cr(CO)_5^-$: 1.80 ± 0.10 eV versus 1.94 ± 0.15 eV (Table III). From the CID data CO can be assigned as the most weakly bound ligand in $Mo(CO)_4O_2^-$ with the Mo–CO bond strength determined to be 0.60 ± 0.05 eV. Remarkably, loss of two CO molecules was not observed at higher energies, but instead $Mo(CO)O_2^-$ ions were detected. The CID results for $Mo(CO)_3O_2^-$ are in good agreement with those of $Mo(CO)_4O_2^-$; that is, $Mo(CO)_2O_2^-$ fragment ions were not observed, whereas generation of $Mo(CO)O_2^-$, i.e. loss of two CO molecules, required 0.42 ± 0.05 eV. Clearly, the Mo–CO bond strength in $Mo(CO)_2O_2^-$ cannot exceed ~0.1 eV. It is noteworthy that the CID data for $Mo(CO)_3O_2^-$ resemble those of $Cr(CO)_3O_2^-$.

Like CrO_5^-, MoO_5^- lost O_2 upon collisional activation. The O_2 binding energy was determined to be 1.52 ± 0.20 eV, 0.19 eV higher than that for the chromium analogue.

C. **Oxidation of $W(CO)_5^-$.** Ionization of a sample containing CH_4 and a small amount of $W(CO)_6$ gave exclusively $W(CO)_5^-$ anions via dissociative electron attachment. Admission of a small amount of O_2 to the sample admitted to the high-pressure source resulted in the generation of a wide variety of oxidized tungsten anions. For a mixture containing 0.8% O_2 the relative abundances of $W(CO)_5^-$, $W(CO)_4O_2^-$, $W(CO)_3O_2^-$, $W(CO)_3O^-$, $W(CO)_2O_2^-$, $W(CO)O_2^-$, WO_5^-, WO_4^-, and WO_3^- were 76, 10, 45, 100, 6, 3, 45, 9, and 11, respectively. At a higher O_2 partial pressure (>1.5%) the WO_4^- and WO_5^- signals dominated the spectrum. With 3.3% O_2 the relative abundances of $W(CO)_4O_2^-$, $W(CO)_3O_2^-$, $W(CO)_3O^-$, WO_5^-, WO_4^-, and WO_3^- were 3, 0.8, 2, 100, 7, and 0.4, respectively. A ratio of 100:38 was obtained for the relative intensities of WO_5^- and WO_4^- at an O_2 content of 59%. These data are in reasonable agreement with the flowing afterglow data presented in Table I.

With an O_2 concentration above 1% relatively weak signals for bimetallic ions, e.g. $W_2O_x^-$ (x = 5–7) were observed as well.

Oxidation of the $W(CO)_5^-$ ions was also examined by trapping them for a variable period of time in the ICR cell in the presence of 5.0×10^{-8} mbar of O_2. $W(CO)_5^-$ was oxidized initially to $W(CO)_3O^-$ and to a lesser extent to $W(CO)_3O_2^-$ (Figure 1C). The latter result is similar to that for the chromium analogue (Figure 1A).

$$W(CO)_5^- + O_2 \rightarrow W(CO)_3O_2^- + 2\,CO \quad (17)$$

$$W(CO)_5^- + O_2 \rightarrow W(CO)_3O^- + CO + CO_2 \quad (18)$$

When $W(CO)_3O^-$ had been trapped for 20 s in the presence of O_2 in the ICR cell the WO_3^- ions represented 31% of the total ion signal.

$$W(CO)_3O^- + O_2 \rightarrow WO_3^- + 3\,CO \quad (19)$$

$W(CO)_3O_2^-$ lost two CO molecules after isolation in the O_2 environment (see below), and the product ion, $W(CO)O_2^-$, was oxidized to WO_3^- and WO_4^-. WO_3^-, WO_4^-, and WO_5^- were inert toward O_2. Thus, the oxidation processes displayed by the chromium and tungsten systems are remarkably similar.

To obtain structural information CID experiments were performed. The CO molecules in $W(CO)_5^-$ were found to be bound by 1.65 ± 0.10 eV, which is less than that for the chromium and molybdenum analogues. Table II shows that none of the $W(CO)_xO_2^-$ ions examined lost O_2 or CO_2 upon collisional activation. $W(CO)_3O_2^-$ is a remarkable species in the sense that ≤0.10 eV is required for loss of two CO molecules (Table III); loss of one CO molecule was not observed. This implies that both $W(CO)_3O_2^-$ and $W(CO)_2O_2^-$ reside in shallow wells on their respective potential energy surfaces. These CID data mimic those for $Cr(CO)_3O_2^-$ and $Mo(CO)_3O_2^-$. Because of the low bond strength the first process observed upon examination of the reactivity of $W(CO)_3O_2^-$ with O_2 is the loss of two CO molecules. It is therefore possible that $W(CO)_3O_2^-$ is inert toward O_2. Although the $W(CO)_4O_2^-$ signal was too weak to allow determination of a threshold for a collision-induced process, the CID process of lowest energy requirement was loss of three CO molecules. The latter result is in qualitative agreement with the data obtained for $W(CO)_3O_2^-$. $W(CO)_3O^-$ lost CO upon collisional activation and the CO binding energy, 1.75 ± 0.05 eV, is close to that for $W(CO)_5^-$ and the similar $Cr(CO)_3O^-$ species.

Like CrO_5^- and MoO_5^-, WO_5^- lost O_2 exclusively upon collisional activation at center-of-mass energies below 5 eV. The O_2 ligand is bound by 1.77 ± 0.15 eV in WO_5^-, which can be compared with 1.33 ± 0.15 eV for CrO_5^- and 1.52 ± 0.20 eV for MoO_5^-.

Discussion

Comparison of the processes involved in oxidation of $Cr(CO)_5^-$, $Mo(CO)_5^-$, and $W(CO)_5^-$ shows some strong similarities, but also some remarkable differences. For example, oxidation of $Cr(CO)_5^-$ did not yield $Cr(CO)_4O_2^-$, and no $Mo(CO)_3O^-$ was observed for reaction of $Mo(CO)_5^-$ with O_2. No rationale is apparent to us to explain these differences.

An interesting question is why MO_5^- was produced upon oxidation in the high-pressure ion source, but not in the low-pressure ICR cell. If it is assumed that the mechanism for generation of MO_5^- is identical for all three group 6 elements, Cr, Mo, and W, then a logical conjecture is that MO_5^- could result from a termolecular reaction, eq 20, in which T is an inert third body.

$$MO_3^- + O_2 + T \rightarrow MO_5^- + T \quad (20)$$

The low pressure in the ICR cell prevents termolecular reactions from taking place and therefore no MO_5^- should be generated. In the flowing afterglow experiments[11] the pressure was lower (0.4 mbar) than in the present experiments (up to 4 mbar) and helium was the carrier gas, which is a less efficient thermalization agent than the CH_4 used here.[26] Thus, MO_5^- generation should be less prominent. Indeed, in the flowing afterglow experiments either MO_5^- was not observed (M = Mo) or MO_5^- was one of many terminal ions. Possibly in disagreement with the mechanism presented above is the observation that for chromium the abundance of CrO_3^- was low and in the case of molybdenum no MoO_3^- was observed. However, the metal–O_2 bond strengths in MO_5^- (see Table III) and the high O_2 pressure in the external ion source suggest fast conversion of MO_3^- to MO_5^-. Alternatively, since $M(CO)_3O_2^-$ was observed for all three group 6 transition metals, it could be the precursor for generation of MO_5^-. In addition, the neutral counterpart of this species played a central role in the photooxidation of $M(CO)_6$ in a solid argon matrix.[9] The following reaction sequence might then also be proposed for the high-pressure ion source:

$$M(CO)_3O_2^- + O_2 \rightarrow M(CO)_xO_3^- + CO_2 + (2-x)\,CO \quad (21)$$

$$M(CO)_xO_3^- + O_2 \rightarrow MO_5^- + x\,CO \quad (22)$$

Indeed, upon careful examination a small amount of $Cr(CO)_2O_3^-$ was detected; with 0.7% O_2 in the mixture the intensity of $Cr(CO)_2O_3^-$ was 0.8% of that of $Cr(CO)_5^-$. The low abundance of the $Cr(CO)_2O_3^-$ signal suggests that it is a rather unstable and/or reactive species. At low pressure in the ICR cell $Cr(CO)_2O_3^-$ loses two CO molecules prior to interaction with O_2, because of insufficient stabilization. (Table III shows that very weak M–CO bonds are not uncommon in these types of species.) In the high-pressure ion source thermalization of ions is efficient. However, intermediates like $M(CO)_xO_3^-$ eluded observation for molybdenum and tungsten upon high-pressure oxidation. Therefore, although no definite conclusions can be drawn concerning the exact mechanism of the formation of MO_5^-, we feel

(26) McEwan, M. J.; Denison, A. B.; Anicich, V. G.; Huntress, W. T. *Int. J. Mass Spectrom. Ion Processes* **1987**, *81*, 247.

that the termolecular mechanism is most likely.

Energy-resolved CID allowed us to assess the bond strengths and the structure of the ions resulting from oxidation of the group 6 metal carbonyl anions. Surprisingly, the order for the metal–CO bond strength in the 17-electron $M(CO)_5^-$ ions, Cr > Mo > W, was found to be the opposite of that found for the neutral 18-electron metal carbonyls, $M(CO)_6$.[27] Table II shows that for all CO-containing product ions, $M(CO)_xO_2^-$ and $M(CO)_yO^-$, the least energy demanding process was loss of one or more CO molecules. The complete absence of O_2 loss from these species suggests that they do not contain an O_2 molecule as a ligand. The latter observation combined with the absence of CO_2 loss implies that dioxo structures are most likely for $M(CO)_4O_2^-$, $M(CO)_3O_2^-$, and $M(CO)O_2^-$, with M having the common oxidation state III. Similar neutral dioxo species have also been observed during photooxidation of $M(CO)_6$ in a solid argon matrix.[9] Significantly, no $Cr(CO)_4O_2$ was generated in the latter matrix isolation experiments, which is in perfect agreement with our results, where $Cr(CO)_4O_2^-$ was not observed. The reduced CO binding energies in $M(CO)_4O_2^-$ and $M(CO)_3O_2^-$ compared to $M(CO)_5^-$ show that the presence of two electron-withdrawing oxygen atoms bound to the metal center weakens the M–CO bond quite severely. The metal–CO bond strengths in the 17-electron $M(CO)_3O_2^-$ ions follow the order Cr > Mo > W, which parallels the order found for the 17-electron $M(CO)_5^-$ ions (see above). Metal–oxo (M=O) bond strengths are known to increase as one moves down the column for the group 6 metals in the periodic table.[24,28]

The loss of O_2 from the terminal MO_5^- product ions upon collisional activation indicates that at least one O_2 molecule must be bound as a peroxo or superoxo ligand in MO_5^-. This is confirmed by the CID data for the ^{18}O-labeled analogues, which show that not all oxygen atoms are equivalent. The latter data also indicate that a structure having two dioxygen (peroxo and/or superoxo) ligands is most likely.[29] Apart from a few porphyrin complexes of chromium, no chromium, molybdenum, and tungsten superoxo complexes are known.[3] Thus, although a superoxo structure cannot be ruled out, we suggest that, by analogy with the stable oxo diperoxo chromium complexes (see Introduction), the MO_5^- ions are oxo diperoxo species as well with the formal oxidation state of the metal atom being V. Loss of O_2 from the latter species could be accompanied by cleavage of the O–O bond of the remaining O_2 ligand. The metal–O_2 bond strength increases from Cr to W, which is in keeping with the increase in metal–ligand bond strengths down the column of the group 6 transition-series metals.[24,27,28]

(27) (a) Lewis, K. E.; Golden, D. M.; Smith, G. P. *J. Am. Chem. Soc.* **1984**, *106*, 3905. (b) Smith, G. P. *Polyhedron* **1988**, *7*, 1605.

(28) Rappé, A. K.; Goddard, W. A., III *J. Am. Chem. Soc.* **1982**, *104*, 3287.

(29) The CID data for $Cr^{16}O_4{}^{18}O^-$ can be used to predict the data for $Cr^{16}O_3{}^{18}O_2^-$. If a CrO_5^- structure is assumed having two dioxygen ligands the ratio for loss of $^{16}O_2$, $^{16}O^{18}O$, and $^{18}O_2$ is predicted to be 20:2:18. However, if the ions would have a structure containing one dioxygen ligand and three separate oxo ligands this ratio would be 16:10:14. The experimental results are most compatible with the former suggestion.

Conclusions

Oxidation of $Cr(CO)_5^-$, $Mo(CO)_5^-$, and $W(CO)_5^-$ was examined in a low-pressure ($\sim 5 \times 10^{-8}$ mbar) and a high-pressure ($\sim$3.5 mbar) environment using a FT-ICR spectrometer equipped with a high-pressure external ion source. Although the oxidation chemistry displayed by the Cr and W systems was fairly similar, the Mo analogue had several unique features. $M(CO)_3O_2^-$ ions and especially $M(CO)_3O^-$ ions were prominent with M = Cr and W under low- and high-pressure conditions. With molybdenum $Mo(CO)_4O_2^-$ was the dominant product ion upon oxidation in the external source. Low-pressure oxidation in the ICR cell yielded $Mo(CO)_3O_2^-$ and to a lesser extent $Mo(CO)_4O_2^-$. Remarkably, MO_5^- ions were only generated under high-pressure conditions. This indicates that generation of MO_5^- ions requires termolecular reactions. Alternatively, it could be that the intermediate for generation of MO_5^- has a very short lifetime and dissociates prior to reaction with O_2 under low-pressure conditions.

Through use of energy-resolved CID experiments the metal–CO bond strengths in $M(CO)_5^-$ were determined to be 1.94 ± 0.15, 1.80 ± 0.10, and 1.65 ± 0.10 eV for M = Cr, Mo, and W, respectively. The latter trend opposes that observed for the metal–CO bond strengths in the neutral group 6 metal carbonyls.[27] CID mass spectra revealed that all the $M(CO)_xO_2^-$ (x = 3, 4) product ions lost one or more CO molecules upon collisional activation. The absence of loss of O_2 and CO_2 suggests that the two oxygen atoms are bound as two separate oxo ligands and not as a dioxygen ligand. Energy-resolved CID showed that the CO molecules in the latter ions are weakly bound and the metal–CO bond strengths follow the same order as that observed for the $M(CO)_5^-$ ions. O_2 loss was the dominant CID process observed for the MO_5^- ions. Thus, two (or possibly one) O_2 molecules must be bound as a peroxo or superoxo ligand in these species. The metal–O_2 binding energies increased down the column of the group 6 transition metals.

Acknowledgment. T.B.M. is grateful to the National Sciences and Engineering Research Council of Canada (NSERC) and the donors of the Petroleum Research Fund, administered by the American Chemical Society, for financial support. The authors also thank R. H. Schultz and Prof. P. B. Armentrout for supplying the CRUNCH program for threshold energy analysis and Prof. L. F. Nazar for helpful discussions.